Published in final edited form as:
Environ Res Lett. 2018 January ; 13(1): . doi:10.1088/1748-9326/aaa00e.

Temperature and humidity based projections of a rapid rise in global heat stress exposure during the 21st century

Ethan D. Coffel[1,3], **Radley M. Horton**[2,3], **Alex de Sherbinin**[4]

[1]Department of Earth & Environmental Sciences, Columbia University

[2]Center for Climate Systems Research, Columbia University

[3]NASA Goddard Institute for Space Studies

[4]Center for International Earth Science Information Network, Columbia University

Abstract

As a result of global increases in both temperature and specific humidity, heat stress is projected to intensify throughout the 21st century. Some of the regions most susceptible to dangerous heat and humidity combinations are also among the most densely populated. Consequently, there is the potential for widespread exposure to wet bulb temperatures that approach and in some cases exceed postulated theoretical limits of human tolerance by mid- to late-century. We project that by 2080 the relative frequency of present-day extreme wet bulb temperature events could rise by a factor of 100 – 250 (approximately double the frequency change projected for temperature alone) in the tropics and parts of the mid-latitudes, areas which are projected to contain approximately half the world's population. In addition, population exposure to wet bulb temperatures that exceed recent deadly heat waves may increase by a factor of five to ten, with 150 – 750 million person-days of exposure to wet bulb temperatures above those seen in today's most severe heat waves by 2070 – 2080. Under RCP 8.5, exposure to wet bulb temperatures above 35°C – the theoretical limit for human tolerance – could exceed a million person-days per year by 2080. Limiting emissions to follow RCP 4.5 entirely eliminates exposure to that extreme threshold. Some of the most affected regions, especially Northeast India and coastal West Africa, currently have scarce cooling infrastructure, relatively low adaptive capacity, and rapidly growing populations. In the coming decades heat stress may prove to be one of the most widely experienced and directly dangerous aspects of climate change, posing a severe threat to human health, energy infrastructure, and outdoor activities ranging from agricultural production to military training.

Introduction

The beginning of the 21st century has seen a variety of extreme heat impacts, from the 2003 European heat wave which was responsible for tens of thousands of additional deaths[1] to the 2010 Russian heat wave which was responsible for a rise in global food prices[2,3]. More recently, extreme temperatures occurred in Australia in 2012 and 2013, the U.S. Southwest in 2013, in India, Pakistan, and other parts of the Middle East in 2015 and 2016[4,5], and again

Author contributions: E.D.C. and R.M.H. jointly conceived the study. E.D.C. conducted the analyses. E.D.C. and R.M.H. jointly wrote the paper. A. de S provided the spatially explicit population projections.

in central Europe in the summer of 2017. Recent attribution studies have suggested that such extreme heat events have already been made more likely due to anthropogenic warming[6–9]. Furthermore, a large body of research now supports the expectation that as the climate continues to warm during the 21st century, the frequency, magnitude, and duration of extreme heat events will increase, as will population exposure to them[10–12]. In many parts of the world, seasonal warming variation may result in the hottest temperatures rising more than the annual mean[13–15] due to proposed mechanisms ranging from land surface interactions[16] to dynamical changes[17]. Recent research has shown that heat extremes directly endanger human life[18], decrease agricultural yields[19], compromise ecosystems[20,21], damage infrastructure[22,23], and impair economic growth[24,25].

Human health impacts depend on both temperature and humidity. The human body is efficient at shedding heat through evaporative cooling, even in high air temperatures, if moisture levels are low. However, in hot and humid conditions the efficiency of evaporative cooling slows and the body may become unable to maintain a stable core temperature. A variety of heat stress indices are used to measure the potential impact of heat on humans. The most common index is the wet bulb globe temperature (WBGT), which is a weighted average of the dry bulb, wet bulb, and mean radiant (globe) temperatures and has a long history of use in the military, athletics, and workplace safety[26]. The WBGT has been shown to have increased along with temperature over the past four decades[27,28]. However, recent research has focused on the standard wet bulb temperature as an indicator of dangerous heat-humidity combinations, and that metric is used in this study. The wet bulb temperature is a physically relevant quantity defined as the temperature that an air parcel would reach through evaporative cooling once fully saturated. When the outside wet bulb temperature exceeds the body's skin temperature, about 35°C, evaporative cooling will be significantly less effective and the body will likely accumulate heat. Prior research has considered this wet bulb temperature threshold to be the limit of human tolerance to heat stress, as in theory a person would eventually suffer heat illness in the absence of artificial cooling[29–31].

Wet bulb temperatures approaching 35°C almost never occur in the current climate[32], and thus there is little real-world data on human health outcomes at the societal level during such extreme conditions. However, recent heat waves with lower wet bulb temperatures between 29°C and 31°C have caused tens of thousands of deaths[5,33], and empirical evidence suggests that most physical labor becomes unsafe at wet bulb temperatures above 32°C[34,35]. Morbidity and mortality can also increase in populations exposed to warm, but not extreme, temperature conditions, as will be commonplace in many areas by the second half of the 21st century[36].The impact of heat stress on human society depends both on the severity of heat waves and the number and vulnerability of people exposed to them. Currently, some regions most at risk for extreme wet bulb temperatures – Northeast India, East China, West Africa, and the Southeast U.S. – are some of the world's most densely populated. In Northeast India and West Africa many people work outdoors and air conditioning, safe water, and medical treatment are not necessarily available. These factors make heat stress much more dangerous, especially for children, the elderly, and people with pre-existing health conditions. Population density is expected to rise dramatically in India and West Africa over the 21st century[37], increasing the number of people exposed to extreme heat at the same time as climate change makes high wet bulb temperature events more severe. In addition,

continued urbanization will place more people in metropolitan areas affected by the urban heat island, which can raise air temperatures by several degrees Celsius[38]. As a result, regardless of whether wet bulb temperatures regularly reach 35°C, extreme heat is poised to become one of the most significant and directly observable impacts of climate change in the coming decades. Global economic impacts can be expected, affecting agriculture, construction, energy demand, emergency services, recreation, and the military[24,25,39,40].

Recent research has increasingly focused on heat stress as a human health risk[35]. The return period of high heat stress events has declined[41] and in the future the frequency of these events may increase the most in the tropics and parts of the mid latitudes that are already hot[27,42]. Two studies have shown that wet bulb temperatures could reach 35°C this century in some locations in the Middle East and India[30,31]. Here we present the first global analysis of population exposure to extreme wet bulb temperatures using 18 general circulation models (GCMs) from the CMIP5[43] suite under two representative concentration pathways (RCP 4.5 & RCP 8.5) along with five spatially explicit population projections from the shared socioeconomic pathways (SSP) project[44]. We calculate future daily air and wet bulb temperatures by adding projected monthly changes from the CMIP5 GCMs onto a present-day air and wet bulb temperature distribution provided by the NCEP Reanalysis II[45]. We partition the rise in exposure into components driven by population increase, climate change, and a combination of the two, and we quantify the uncertainty associated with each.

Data and Methods

We calculate daily maximum wet bulb temperatures for the NCEP Reanalysis II[45] and 18 CMIP5 GCMs using the daily maximum air temperature, daily mean specific humidity, and daily mean surface pressure using the algorithm described in Davies-Jones (2008)[46], implemented by Buzan (2015)[35], and ported to Matlab by Dr. Robert Kopp (Rutgers, 2016). The reanalysis and GCM data are re-gridded using linear interpolation to a 2°×2° resolution to facilitate spatial comparison. Using the daily maximum temperature as opposed to a six-hourly time step in wet bulb temperature calculations prevents an underestimation of the daily maximum temperature due to it falling in between two of the time steps. Future changes in monthly-mean daily maximum temperature and wet bulb temperature, relative to 1985 – 2005, are calculated at each grid cell for each GCM and emission scenario in each year between 2020 and 2080. These projected monthly changes are added to the historical daily maximum temperatures and wet bulb temperatures taken from the NCEP Reanalysis II for the period 1985 – 2005, generating a set of daily future projections which retain reanalysis-based historical daily variability and spatial patterns. This method eliminates GCM mean bias, although such mean biases may affect the warming simulated by GCMs and thus the projections used here. Variations in the spatial distribution, seasonality, or sub-monthly variability of warming could act to either increase or decrease projected future wet bulb temperatures. In addition, any errors in the original reanalysis will be retained. However, given the need for projections of absolute wet bulb temperature, we consider this method preferable to bias-correcting GCM temperature and humidity data, as such corrections can produce non-physical results. The NCEP Reanalysis II is most accurate in regions with dense observational weather data; NCEP II historical period wet bulb temperatures are compared with daily maximum wet bulb temperatures computed using

observed station data in a variety of countries, some with dense station data networks (such as the U.S. or Germany) and others with sparse ground observations (such as Nigeria and parts of rural Brazil) (Supplementary Figure 2). The bias between NCEP II and station data is between 0 and negative 3°C (indicating that the NCEP II is too cool), with most regions experiencing biases closer to negative 1°C. These negative biases suggest that our wet bulb temperature projections may be somewhat conservative in these regions. We elect not to bias-correct the NCEP II dataset due to varying and uncertain quality and consistency in observed station data.

We calculate the relative frequency of future heat events for each GCM grid cell as the mean number of days per year during 2060 – 2080 which exceed the mean annual maximum temperature and wet bulb temperature for the same GCM during the modeled 1985–2005 period.

Spatially explicit population projections from the SSP project are up-scaled to a 2°×2° degree latitude/longitude grid to match the GCM resolution, and population exposure to wet bulb temperature thresholds are calculated for each GCM separately at a daily time resolution. If the GCM wet bulb temperature at a given grid cell exceeds a threshold value (e.g a wet bulb of 32°C or 35°C) on a given day, the grid cell is considered exposed, and the population total for that grid cell is added to the person-day exposure count. The annual exposure totals (in person-days) can count the same people multiple times, and indeed do as much of the exposure to high wet bulb temperatures occurs in the same grid cells repeatedly.

The population exposure values are decomposed into three components: the population effect, the climate effect, and the combined effect. The population effect is calculated as the exposure in person-days that would result from a changing population under a constant climate. The historical daily maximum wet bulb temperatures (1985 – 2005) are used to select exposed grid cells, and mean population exposure for each decade is computed using decadal population means from the five SSP scenarios. Uncertainty in the population effect is estimated by taking the full range across the five SSPs, and this is displayed as the error bar on the population effect bars in Figure 3b–c. The climate effect is the exposure that results from rising temperatures alone, holding population constant (using SSP estimated population data from 2010). Uncertainty in the climate effect is calculated by taking the 10^{th} – 90^{th} percentile range across the 18 GCMs (so as to reduce the effect of outlier temperature change projections in several GCMs). The combined effect is calculated as the total population exposure minus the population and climate effects, and the uncertainty bars show the 10^{th} – 90^{th} percentile range across five SSPs and 18 GCMs. This represents the exposure that results from both rising populations and rising temperatures.

Results and Discussion

The changes in wet bulb temperatures are expected to be smaller, more spatially uniform, and have less inter-GCM variation than for air temperatures, as GCMs that project the largest increases in air temperature also project the largest decreases in relative humidity, producing a stabilizing effect on wet bulb temperature projections[47]. By 2070 – 2080, we project global multi-GCM mean increases in annual maximum wet bulb temperature across

the tropics and mid-latitudes of 2 – 3°C (Figure 1d–e), with an inter-GCM range from 1 – 2.5°C under RCP 4.5 and 2 – 4.5°C under RCP 8.5. These projected increases are similar to those found in other studies focused on regional wet bulb temperature changes[30,31].

Annual maximum wet bulb temperatures are projected to increase by approximately the same amount as mean daily maximum wet bulb temperatures across the tropics and mid-latitudes. This stands in contrast to annual maximum air temperatures, which are projected to increase by 1 – 2°C more than mean daily maximum temperatures in many regions, notably in the eastern U.S., much of Europe, the Middle East and India, and eastern China (Supplementary Figure 9). This divergence between changes in mean and extreme air temperatures aligns with previous research[13–15,48] and may be driven by land-atmosphere interactions and dynamical changes[11,16,17].

As global mean temperatures warm, it is expected, and has been observed, that atmospheric specific humidity levels will rise in accordance with the Clausius-Clapeyron relation[49], with the largest increases in specific humidity expected over the oceans. Four regions particularly vulnerable to heat stress, the eastern U.S., northeastern India, eastern China, and West Africa, have different climates and synoptic patterns during heat waves which affect the relative importance of temperature and humidity as contributors to extreme wet bulb temperatures. We find that on the days with the highest wet bulb temperatures, specific humidity increases of 10 – 15% (relative to high wet bulb temperature days in the historical period) are projected across all four regions. However, increases in temperature on the days with the highest wet bulb temperatures range from 1 – 2°C in India to 3 – 4°C in the eastern U.S., West Africa, and eastern China (see Supplementary Figure 3), driving the regional differences in wet bulb temperature change.

Populations are to a large extent adapted to their local climates. To assess how wet bulb temperatures will change relative to historical conditions we project the number of days per year that may exceed the historical annual maximum air and wet bulb temperatures. By 2060 – 2080, most regions within 30° latitude of the equator may experience between 25 and 150 days per year that exceed the historical once-per-year maximum air temperature, and 25 – 250 days per year that exceed historical once-per-year maximum wet bulb temperature (Figure 2). In the mid-latitudes, these numbers are somewhat lower at 25 – 40 days per year for both air and wet bulb temperature, due to higher baseline variability. These results suggest a radical transformation of tropical and sub-tropical heat environments, with much of the year being spent above the highest historical wet bulb temperatures. As the duration of heat exposure is essential in determining health impacts, more research is needed into the potential mortality response associated with long duration (months) heat exposure interspersed with unprecedented extreme heat waves.

Substantial population growth is expected throughout the 21st century, especially in the developing world (Supplementary Figure 7). Much of this growth is anticipated to occur in regions that experience high wet bulb temperatures, resulting in large increases in the number of people exposed to dangerous heat conditions. We estimate annual exposure in terms of person-days (one person exposed on one day) to high wet bulb temperatures in each decade through 2080 using the SSP population projections (Figure 3). We estimate a broad

range of exposure uncertainty by combining 18 GCMs and five SSPs under two emissions scenarios, assuming that the uncertainty resulting from GCM variability, future emissions trajectories, and population growth are equally irreducible in the context of present-day decision-making. Our results include repeat exposures (see Supplementary Figure 5 for the spatial distribution of exposure), and as the highest wet bulb temperatures are concentrated in a few regions, the same populations will likely bear the brunt of the world's most extreme heat.

Exposure to extreme wet bulb temperatures depends heavily on future greenhouse gas emissions. Figure 3a shows the projected mean annual exposure to wet bulb temperatures from 30 – 35°C across 18 GCMs and five SSPs under RCP 4.5 and RCP 8.5. Projected exposure under the two emissions scenarios sharply diverges above wet bulb temperatures of approximately 32°C, the temperature above which most sustained labor becomes impossible[34,35], with differences in exposure person-days of several orders of magnitude. Figure 3b and 3c show projected exposure to wet bulb temperatures above 32°C, above the highest commonly experienced in the historical climate. By the 2070s annual exposure to wet bulb temperatures of at least 32°C may increase by a factor of 5 – 10 (relative to 2020; 32°C wet bulb temperatures are extremely rare in the 1985 – 2005 period) to around 750 million person days under RCP 8.5 and 250 million person days under RCP 4.5 (Figure 3b, c; see Supplementary Figure 4 for full exposure results). Under the RCP 8.5 scenario, in any given year during the 2070s we project that there is a greater than 33% chance of a wet bulb temperature above 34°C occurring in at least one model grid cell, and a greater than 15% chance for a wet bulb temperature above 35°C (Supplementary Figure 6). These extreme wet bulb temperatures are concentrated in small parts of India, China, and the Amazon (Supplementary Figure 5), but due to the high population densities in India and China, our results suggest multi-model mean annual exposure to wet bulb temperatures of 35°C or higher to be approximately a million person-days by the 2070s under RCP 8.5. The uncertainty range in exposure at all thresholds results mostly from differences in projected warming and moistening between GCMs and emissions scenarios, with a smaller contribution from population variation among SSPs.

We divide global population exposure into three components[12]: the population effect, or the additional exposure driven entirely by population growth (a constant climate but growing population); the climate effect, the exposure driven by climate change (constant population but changing climate); and the combined effect, or the exposure that results from changing population and changing climate in the same location (e.g. the additional exposure that results from both population growth and climate change). The combined effect is equal to the total exposure minus the population and climate effects. Globally, the population effect is near zero as the vast majority of additional exposure is due to climate change; wet bulb temperatures of 31°C and higher are rare in the current climate and would remain so without warming. However, the combined effect comprises a substantial portion of increased exposure, indicating that while climate change is the dominant factor in increasing future exposure, population growth in hot regions also plays an important role.

Recent research suggests that there is no fundamental cap on wet bulb temperature[50–52]. However, further research into the development of convection at high wet bulb temperatures

and tropical thermodynamics, including changes in vertical potential temperature profiles, extreme SSTs, and SST gradients, is warranted, as is further evaluation of GCM simulations of expected physical processes in a warmer future climate. It is possible that achieving high wet bulb temperatures may depend on strong local atmospheric subsidence inhibiting convection, but this process is not represented in GCMs; higher resolution, convection-resolving models could help resolve this question. Recent research has hinted at the possibility that shifts in dynamic (e.g. atmospheric blocking) and thermodynamic (e.g. soil moisture) processes poorly simulated by GCMs may be modifying the statistics of extreme temperatures, but the implications for extreme wet bulb temperatures remain unexplored. In general there is a negative correlation between warming and relative humidity change over interior continents[47] as dryer conditions result in more efficient warming of the air. However, research suggests that some localized heat stress hot spots, especially in the coastal Middle East, may result from the interaction of hot desert air masses with onshore moisture advection from warm bodies of water[30]; these processes occur at too small a scale to be captured by GCMs, potentially adding a conservative bias to our results if they occur in other regions in the future. Further research is also needed into regional influences on heat, such as topography, local synoptic patterns, and the urban heat island effect, and whether variability of wet bulb temperatures may change on a daily timescale. In addition, given that small differences in wet bulb temperature can lead to large differences in population exposure to dangerous heat, GCM bias may have an important effect on projected results; advanced methods of GCM bias correction[53] could be tested and compared with the reanalysis-based projection method presented here.

Our initial exploration of a potentially transformative risk factor for humans only considers population exposure. However, the impacts of heat on humans depend on both exposure and vulnerability, with the latter depending on many other factors including population age, degree and type of pre-existing health conditions, acclimatization, adaptive capacity, access to air conditioning, emergency response to severe heat waves, and economic and sociocultural factors that influence behavior[54]. In addition, research has shown that relatively simple adaptation strategies such as early warning of heat waves, public education campaigns on the dangers of heat, and social check-ups on vulnerable people can drastically reduce the death toll on hot days[33,55]. Each dimension of vulnerability will shape the impacts of heat stress events in distinct ways, pointing at the need for deeper epidemiological and economic analyses. We also only consider heat stress at a 2° spatial resolution – the urban heat island and other localized climate effects could result in locally higher wet bulb temperatures than are represented by the grid cell-average.

There is high uncertainty in the population projections that we consider in this study, and the five SSPs are not independent from future emission scenarios (i.e. higher population is likely associated with higher emissions). However, as a warming climate is by far the largest contributor to increasing heat exposure, changes in the future population trajectory are projected to have a second-order effect. The SSPs may offer a means of exploring potentially critical correlations between heat, population density, vulnerability, and the potential for adaptation. Furthermore, the potential for non-linear increases in impacts at the highest wet bulb temperatures suggest the need for further research into the characteristics of heat events, such as duration and potential correlation with co-hazards such as air pollution,

dehydration, and sun exposure. The effects of rapid increases in wet bulb temperature on ecosystems and wildlife, especially large mammals, should also be considered.

Our results suggest that exposure to extreme wet bulb temperatures will rapidly increase throughout the 21st century and potentially beyond, depending on future greenhouse gas emissions. Given the number of people who may be exposed to dangerous heat across the world, failure to adopt both mitigation and adaptation measures is likely to result in suffering, economic damage, and increased heat-related mortality.

Supplementary Material

Refer to Web version on PubMed Central for supplementary material.

Acknowledgments

We acknowledge the World Climate Research Programme's Working Group on Coupled Modelling, which is responsible for CMIP, and we thank the climate modeling groups for producing and making available their model output. For CMIP the U.S. Department of Energy's Program for Climate Model Diagnosis and Intercomparison provides coordinating support and led development of software infrastructure in partnership with the Global Organization for Earth System Science Portals. Funding for this research was provided through NSF grant number DGE-11-44155 and the US DOI. We would also like to acknowledge Bryan Jones of Baruch College, who provided access to the population projections used in this article.

References

1. Haines A, Kovats RS, Campbell-Lendrum D & Corvalan C Climate change and human health: Impacts, vulnerability and public health. Public Health 120, 585–596 (2006). [PubMed: 16542689]
2. Dole R et al. Was there a basis for anticipating the 2010 Russian heat wave? Geophys. Res. Lett 38, (2011).
3. Welton G The Impact of Russia' s 2010 Grain Export Ban. Oxfam Res. Reports 32 (2011).
4. Ghumman U & Horney J Characterizing the Impact of Extreme Heat on Mortality, Karachi, Pakistan, June 2015. Prehosp. Disaster Med 31, 263–6 (2016). [PubMed: 27046134]
5. Zommers Z et al. Loss and Damage: The Role of Ecosystem Services. (United National Environment Programme, 2016).
6. Christidis N, Jones GS & Stott PA Dramatically increasing chance of extremely hot summers since the 2003 European heatwave. Nat. Clim. Chang 5, 3–7 (2015).
7. Stott PA, Stone DA & Allen MR Human contribution to the European heatwave of 2003. Nature 432, 610–614 (2004). [PubMed: 15577907]
8. Rahmstorf S & Coumou D Increase of extreme events in a warming world. Proc. Natl. Acad. Sci 109, 4708–4708 (2012).
9. Black E, Blackburn M, Harrison RG, Hoskins BJ & Methven J Factors contributing to the summer 2003 European heatwave. Weather 59, 217–223 (2004).
10. Meehl GA & Tebaldi C More Intense, More Frequent, and Longer Lasting Heat Waves in the 21st Century. Science (80-.) 305, 994–997 (2004).
11. Horton RM, Mankin JS, Lesk C, Coffel E & Raymond C A Review of Recent Advances in Research on Extreme Heat Events. Curr. Clim. Chang. Reports 2, 242–259 (2016).
12. Jones B et al. Future population exposure to US heat extremes. Nat. Clim. Chang 5, 652–655 (2015).
13. Kodra E & Ganguly AR Asymmetry of projected increases in extreme temperature distributions. Sci. Rep 4, 5884 (2014). [PubMed: 25073751]
14. Horton RM, Coffel ED, Winter JM & Bader DA Projected changes in extreme temperature events based on the NARCCAP model suite. Geophys. Res. Lett 42, 7722–7731 (2015).

15. Argüeso D, Luca A Di, Perkins-Kirkpatrick, S. E. & Evans, J. P. Seasonal mean temperature changes control future heat waves. Geophys. Res. Lett (2016). doi:10.1002/2016GL069408
16. Miralles DG, Teuling AJ, van Heerwaarden CC & Vilà-Guerau de Arellano J Mega-heatwave temperatures due to combined soil desiccation and atmospheric heat accumulation. Nat. Geosci 7, 345–349 (2014).
17. Coumou D, Petoukhov V, Rahmstorf S, Petri S & Schellnhuber HJ Quasi-resonant circulation regimes and hemispheric synchronization of extreme weather in boreal summer. Proc. Natl. Acad. Sci 111, 12331–12336 (2014). [PubMed: 25114245]
18. Petkova EP, Horton RM, Bader DA & Kinney PL Projected heat-related mortality in the U.S. Urban Northeast. Int. J. Environ. Res. Public Health 10, 6734–6747 (2013). [PubMed: 24300074]
19. Hatfield J et al. Ch. 6: Agriculture. in Climate Change Impacts in the United States: The Third National Climate Assessment (eds. Melillo JM, (T.C.), T. R. & Yohe GW) 150–174 (U.S. Global Change Research Program, 2014).
20. Kurz WA et al. Mountain pine beetle and forest carbon feedback to climate change. Nature 452, 987–990 (2008). [PubMed: 18432244]
21. Lesk C, Coffel E, D'Amato AW, Dodds K & Horton R Threats to North American forests from southern pine beetle with warming winters. Nat. Clim. Chang (2017). doi:10.1038/nclimate3375
22. Coffel E & Horton R Climate Change and the Impact of Extreme Temperatures on Aviation. Weather. Clim. Soc 7, 94–102 (2015).
23. Coffel ED, Thompson TR & Horton RM The impacts of rising temperatures on aircraft takeoff performance. Climatic Change 1–8 (2017). doi:10.1007/s10584-017-2018-9
24. Kjellstrom T, Kovats RS, Lloyd SJ, Holt T & Tol RSJ The Direct Impact of Climate Change on Regional Labor Productivity. Arch. Environ. Occup. Health 64, 217–227 (2009). [PubMed: 20007118]
25. Dunne JP, Stouffer RJ & John JG Reductions in labour capacity from heat stress under climate warming. Nat. Clim. Chang 3, 563–566 (2013).
26. Budd GM Wet-bulb globe temperature (WBGT)-its history and its limitations. J. Sci. Med. Sport 11, 20–32 (2008). [PubMed: 17765661]
27. Willett KM & Sherwood S Exceedance of heat index thresholds for 15 regions under a warming climate using the wet-bulb globe temperature. Int. J. Climatol 32, 161–177 (2012).
28. Knutson TR & Ploshay JJ Detection of anthropogenic influence on a summertime heat stress index. Clim. Change 138, 25–39 (2016).
29. Sherwood SC & Huber M An adaptability limit to climate change due to heat stress. Proc. Natl. Acad. Sci 107, 9552–9555 (2010). [PubMed: 20439769]
30. Pal JS & Eltahir EAB Future temperature in southwest Asia projected to exceed a threshold for human adaptability. Nat. Clim. Chang 18203, 1–4 (2015).
31. Im E-S, Pal JS & Eltahir EAB Deadly heat waves projected in the densely populated agricultural regions of South Asia. Sci. Adv 3, 1–8 (2017).
32. Schar C Climate extremes: The worst heat waves to come. Nat. Clim. Chang 6, 128–129 (2016).
33. Fouillet A et al. Has the impact of heat waves on mortality changed in France since the European heat wave of summer 2003? A study of the 2006 heat wave. Int. J. Epidemiol 37, 309–317 (2008). [PubMed: 18194962]
34. Liang C et al. A new environmental heat stress index for indoor hot and humid environments based on Cox regression. Build. Environ 46, 2472–2479 (2011).
35. Buzan JR, Oleson K & Huber M Implementation and comparison of a suite of heat stress metrics within the Community Land Model version 4.5. Geosci. Model Dev 8, 151–170 (2015).
36. Kjellstrom T, Gabrysch S, Lemke B & Dear K The 'Hothaps' programme for assessing climate change impacts on occupational health and productivity: an invitation to carry out field studies. Glob. Health Action 2, 10.3402/gha.v2i0.2082 (2009).
37. World Population Prospects The 2012 Revision Volume I : Comprehensive Tables. 1, (United Nations Population Division, 2013).
38. Zhao L, Lee X, Smith RB & Oleson K Strong contributions of local background climate to urban heat islands. Nature 511, 216–219 (2014). [PubMed: 25008529]

39. Kjellstrom T, Holmer I & Lemke B Workplace heat stress, health and productivity – an increasing challenge for low and middle-income countries during climate change. Glob. Health Action 2, 10.3402/gha.v2i0.2047 (2009).
40. Burke M, Hsiang SM & Miguel E Global non-linear effect of temperature on economic production. Nature 527, 235–239 (2015). [PubMed: 26503051]
41. Sippel S & Otto FEL Beyond climatological extremes - assessing how the odds of hydrometeorological extreme events in South-East Europe change in a warming climate. Clim. Change 125, 381–398 (2014).
42. Battisti DS & Naylor RL Historical Warnings of Future Food Insecurity with Unprecedented Seasonal Heat. Science (80-.) 323, 240–244 (2009).
43. Taylor KE, Stouffer RJ & Meehl GA An overview of CMIP5 and the experiment design. Bull. Am. Meteorol. Soc 93, 485–498 (2012).
44. O'Neill BC et al. A new scenario framework for climate change research: The concept of shared socioeconomic pathways. Clim. Change 122, 387–400 (2014).
45. Kanamitsu M et al. NCEP–DOE AMIP-II Reanalysis (R-2). Bull. Am. Meteorol. Soc 83, 1631–1643 (2002).
46. Davies-Jones R An Efficient and Accurate Method for Computing the Wet-Bulb Temperature along Pseudoadiabats. Mon. Weather Rev 136, 2764–2785 (2008).
47. Fischer EM & Knutti R Robust projections of combined humidity and temperature extremes. Nat. Clim. Chang 3, 126–130 (2012).
48. Ballester J, Rodó X & Giorgi F Future changes in Central Europe heat waves expected to mostly follow summer mean warming. Clim. Dyn 35, 1191–1205 (2010).
49. Willett KM, Gillett NP, Jones PD & Thorne PW Attribution of observed surface humidity changes to human influence. Nature 449, 710–712 (2007). [PubMed: 17928858]
50. Williams IN, Pierrehumbert RT & Huber M Global warming, convective threshold and false thermostats. Geophys. Res. Lett 36, 2–6 (2009).
51. Frieling J et al. Extreme warmth and heat-stressed plankton in the tropics during the Paleocene-Eocene Thermal Maximum. Sci. Adv 3, e1600891 (2017). [PubMed: 28275727]
52. Korty RL, Emanuel KA, Huber M & Zamora RA Tropical cyclones downscaled from simulations with very high carbon dioxide levels. J. Clim 30, 649–667 (2017).
53. Levy AAL et al. Can correcting feature location in simulated mean climate improve agreement on projected changes? Geophys. Res. Lett 40, 354–358 (2013).
54. Luber G & McGeehin M Climate Change and Extreme Heat Events. Am. J. Prev. Med 35, 429–435 (2008). [PubMed: 18929969]
55. Vandentorren S et al. August 2003 heat wave in France: Risk factors for death of elderly people living at home. Eur. J. Public Health 16, 583–591 (2006). [PubMed: 17028103]

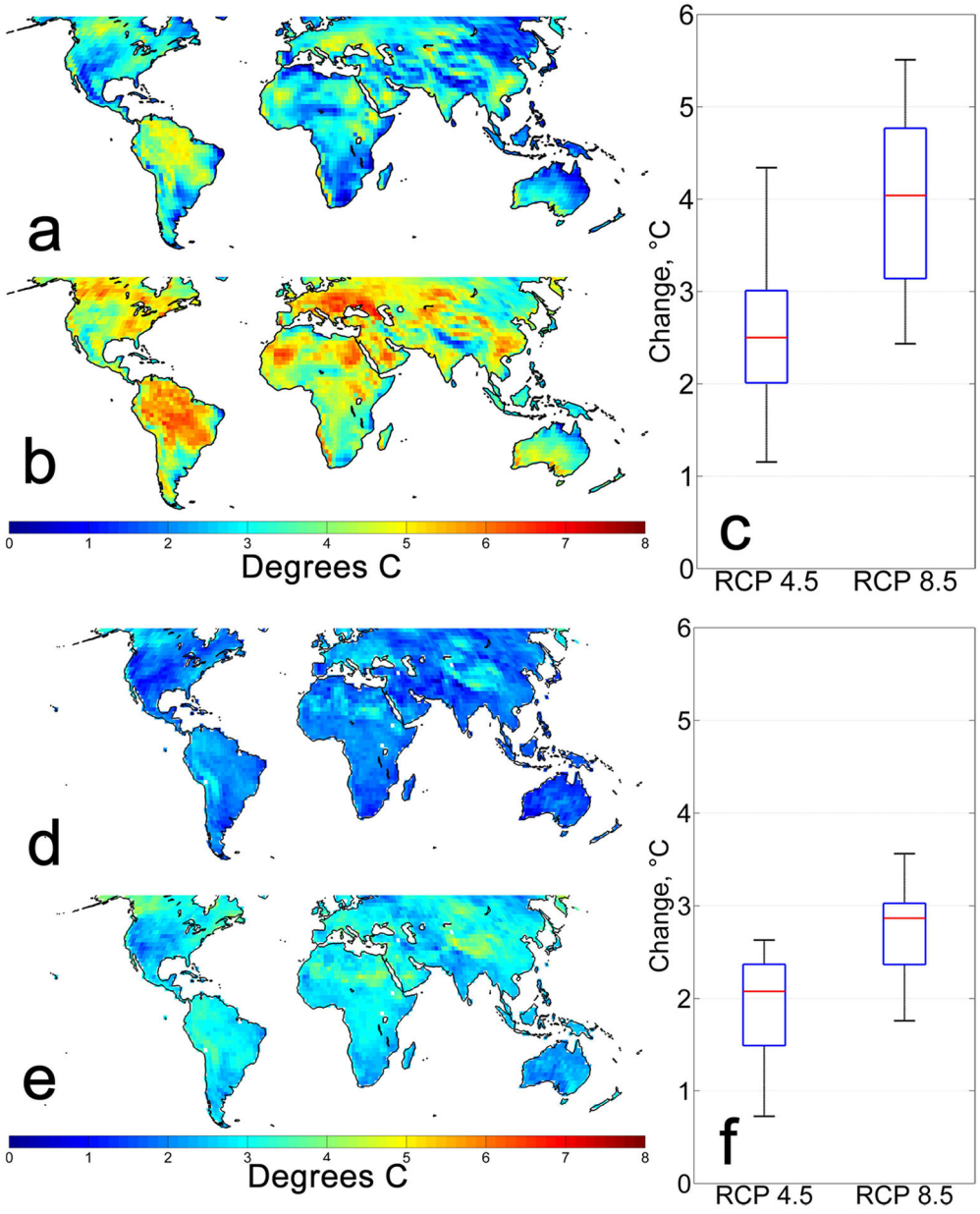

Figure 1:

Top panel (a-c): changes in annual maximum air temperature in 2060 – 2080 relative to 1985 – 2005 under RCP 4.5 (a) and RCP 8.5 (b). Panel (c) shows the range in projected annual maximum temperature increase spatially averaged over land for both emission scenarios over all 18 CMIP5 GCMs. Bottom panel (d-f): same as (a-c) except for annual maximum wet bulb temperature. Air temperatures increase at a faster rate and have more spatial variability than wet bulb temperatures, in part due to the dependence of wet bulb temperature on humidity.

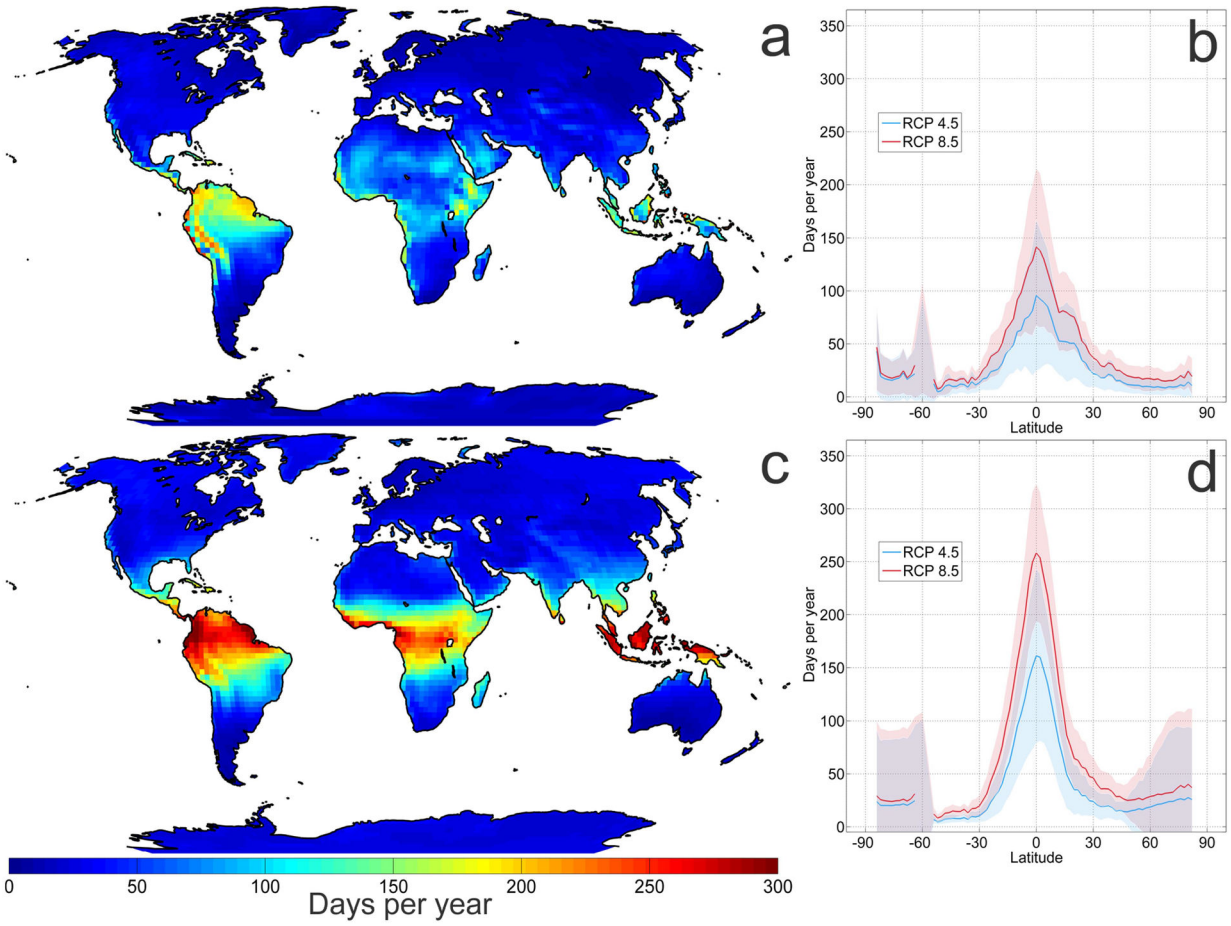

Figure 2:

The number of days per year which exceed the historical (1985–2005) mean annual maximum temperature (top row) and wet bulb temperature (bottom row) in 2060 – 2080. Maps show results under RCP 8.5 (see Supplementary Figure 8 for maps under RCP 4.5), and (b, d) show the variation with latitude of the number of days per year under both RCP 4.5 and RCP 8.5, excluding water grid cells. Wet bulb temperatures exceed the historical mean annual maximum more frequently than air temperatures due to lower variability, especially in the tropics.

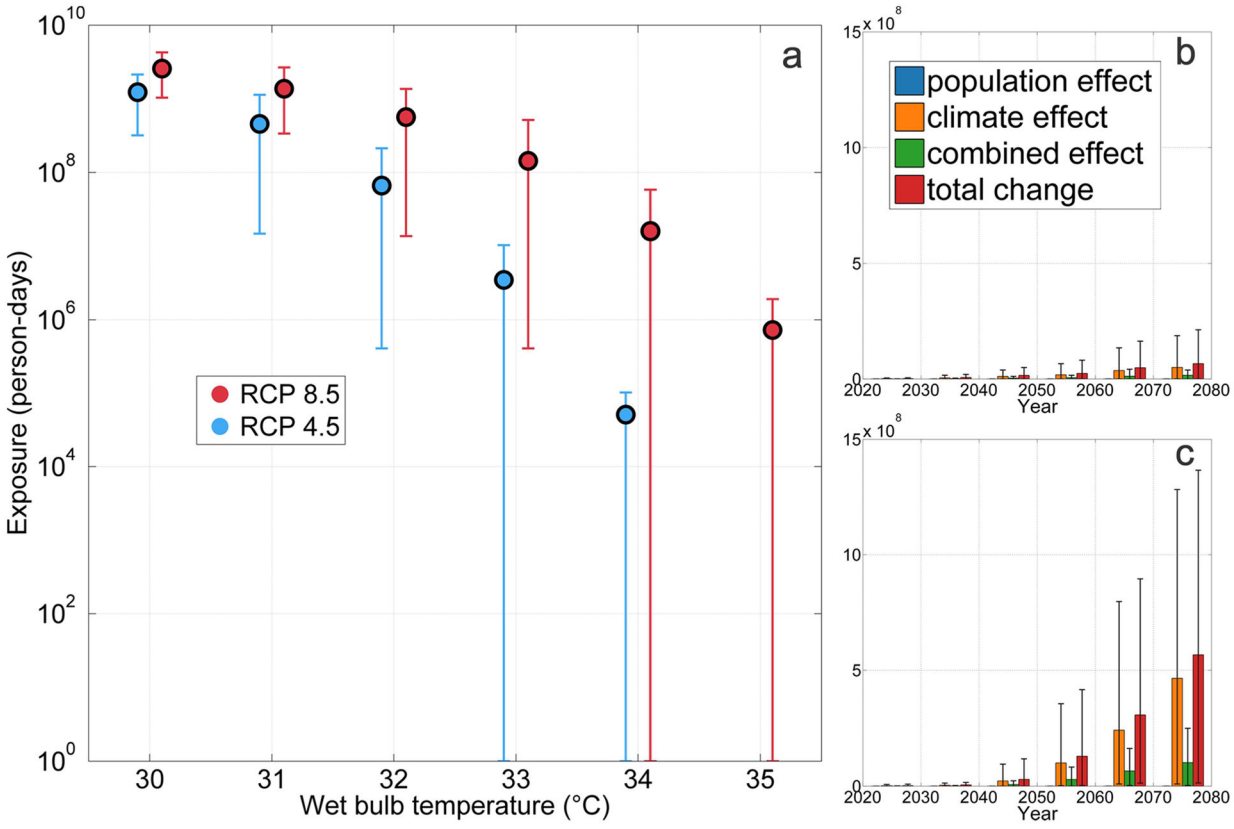

Figure 3:

Global population exposure to varying wet bulb temperature thresholds, in mean number of person-days per year. (a): Global mean annual exposure under RCP 4.5 and RCP 8.5 in 2070 – 2080 to wet bulb temperatures from 30 – 35°C. Error bars show the full range across 18 GCMs and five SSPs. Exposure to wet bulb temperatures above 30°C is reduced by several orders of magnitude in RCP 4.5 as compared to RCP 8.5. Right: mean global annual exposure to wet bulb temperatures exceeding 32°C, approximately the upper limit at which sustained physical labor is possible[34] and above anything experienced in the historical climate. RCP 4.5 is shown on top (b), and RCP 8.5 on bottom (c). Exposure is separated into a population effect (constant climate but changing population), climate effect (constant population but changing climate), and a combined effect (result of changing population and changing climate). Total exposure is the sum of these three components. Error bars on total exposure show the 10^{th} – 90^{th} percentile range across 18 GCMs and five SSPs.

Table 1:

Selected CMIP5 GCMs.

Model	Organization	Native Resolution
ACCESS1–0	Commonwealth Scientific and Industrial Research Organisation	1.25° × 1.875°
ACCESS1–3	Commonwealth Scientific and Industrial Research Organisation	1.25° × 1.875°
BCC-CSM1–1-M	Beijing Climate Center	2.7906° × 2.8125°
BNU-ESM	College of Global Change and Earth System Science, Beijing, Normal University	2.7906° × 2.8125°
CANESM-2	Canadian Centre for Climate Modelling and Analysis	2.7906° × 2.8125°
CSIRO-MK3-6-0	Commonwealth Scientific and Industrial Research Organisation	1.8653° × 1.875°
CNRM-CM5	Centre National de Recherches Meteorologiques / Centre Europeen de Recherche et Formation Avancee en Calcul Scientifique	1.4008° × 1.40625°
FGOALS-G2	State Key Laboratory for Numerical Modeling for Atmospheric Science and Geophysical Fluid Dynamics	2.7906° × 2.8125°
GFDL-CM3	NOAA Geophysical Fluid Dynamics Laboratory	2.0° × 2.5°
GFDL-ESM2G	NOAA Geophysical Fluid Dynamics Laboratory	2.0225° × 2.0°
GFDL-ESM2M	NOAA Geophysical Fluid Dynamics Laboratory	2.0225° × 2.5°
HADGEM2-CC	Met Office Hadley Center	1.25° × 1.875°
HADGEM2-ES	Met Office Hadley Center	1.25° × 1.875°
IPSL-CM5A-MR	Institut Pierre-Simon Laplace	1.2676° × 2.5°
IPSL-CM5B-LR	Institut Pierre-Simon Laplace	1.8947° × 3.75°
MIROC5	International Centre for Earth Simulation	1.4008° × 1.40625°
MRI-CGCM3	Meteorological Research Institute	l.12148° × 1.125°
NORESM1-M	Norwegian Climate Centre	1.8947° × 2.5°